Astronomical and Astrophysical Transactions, 1996,
Vol. 10, pp. 225–233
Reprints available directly from the publisher
Photocopying permitted by license only

ASTROPHYSICS

LARGE-SCALE STRUCTURES IN THE ISM WITH CORRELATED SNe EXPLOSIONS

S. A. SILICH and S. Ya. MASHCHENKO

Main Astronomical Observatory of the National Academy of Sciences of Ukraine
252650, Kiev, Goloseevo, Ukraine

(Received October 19, 1994)

Hydrodynamics of the expanding interstellar shells caused by correlated SNe explosions in different galactic environments is considered. Action of the galactic shear, gravity and inhomogeneities of the interstellar medium are discussed. The results of the 2.5D numerical simulations of superbubble evolution in our Galaxy and in the irregular galaxy HoII are compared with observational data. The distribution of major axes of superbubbles in the inner part of the HoII galaxy is assumed to be the result of the huge shells collisions or interaction with the diffuse interstellar clouds.

KEY WORDS Interstellar matter

1 INTRODUCTION

This conference is devoted to the memory of the prominent scientist G. Gamow. He is well known as the author of the "Big Bang" theory – the theory of the origin and evolution of the Universe. We shall concentrate in our presentation on the explosion phenomena too, but on a shorter characteristic scale. We shall discuss evolution of expanding interstellar shells in different galactic environments. These objects were first recognized in the Small Magellanic Cloud (SMC) by Hindman (1967) and then discovered in our own Galaxy by the American astrophysicist Heiles (1979). Now expanding shells, supershells, bubbles, and regions with deficient interstellar matter are observed in almost all energy bands: from radio and IR to the visible H_α, OIII lines and to extended regions of soft X-ray emission. A shell-like structure of the ISM has been revealed during the last decade in almost all nearby galaxies which have been observed with a high space and energy resolution (for more details see reviews by Tenorio-Tagle and Bodenheimer, 1988 and Brinks, 1990). The characteristic scale of the shells is (0.1–1) kpc, they cover up to 15% of the whole surface of the galactic disk and belong to the most extensive features in the galaxies. The kinetic energies of the expanding shells reach in some cases 10^{53} ergs and they seem

Table 1. The energy characteristics of different astrophysical objects

Object	*Energy*
Single supernova explosion	$\approx 10^{51}$ ergs
Interstellar bubbles and superbubbles	$\approx 10^{54}$ ergs
Galaxies with the starbust activity	$\approx 10^{56}$ ergs
Radiogalaxies and quasars	$\approx 10^{60}$ ergs

to fill the energy gap between single supernova explosions and starbust galaxies (see Table 1).

Thus expanding shells and supershells define the large-scale dynamics and energy balance of the ISM, the disk-halo connection, the enrichment of the ISM by the heavy elements, the redistribution of the galactic gas among different phases (molecular, neutral, ionized) of the interstellar medium and can stimulate the process of star formation.

There are two basic mechanisms for the origin of the huge expanding shells which are currently under discussion. The first one is the supernova explosions correlated in space. Cox and Smith (1974) were the first who recognized that the hot gas from supernova explosions is long lived. Thus repeated explosions of massive stars within the preexisting cavity should create huge expanding bubbles of the hot rarefied gas and compress ambient interstellar gas into a dense expanding shell. This picture was developed later by Tomisaka *et al.* (1981), McCray and Kafatos (1987) and many others, and it is based on the fact that most of the massive luminous stars are born in huge groups in separated regions and are organized in OB-associations, or, on large scales, in star complexes (Efremov, 1978; Elmegreen, 1985). An alternative explanation was proposed by Tenorio–Tagle (1980), Tenorio–Tagle *et al.* (1986), who considered impact of massive high-velocity clouds with the galactic disk.

We shall consider the first mechanism which operates in many objects. We assume a continuous energy release rate during $\approx$30 Myrs (the lifetime of an OB-association) in a region of space due to coherent supernova explosions in an OB-association.

There are two main dynamic effects which act on the bubble expansion: inhomogeneity of the gas density distribution in the direction normal to the galactic plane and differential galactic rotation. Therefore three-dimensional calculations should be provided for adequate simulation of the bubble evolution. The three-dimensional numerical schemes based on the thin layer approximation (2.5-dimensional hydrodynamics) have been developed by Palous (1990), Bisnovatyi–Kogan and Silich (1991) and Silich (1992).

The growing bulk of observational data and development of the new numerical hydrodynamic schemes allow to develop a more comprehensive scenario to the evolution of the large-scale structures in the ISM and to compare the existing theoretical models with the observed properties of the interstellar gas, in particular, with some statistical features of the distribution of HI holes and shells in the nearby galaxies.

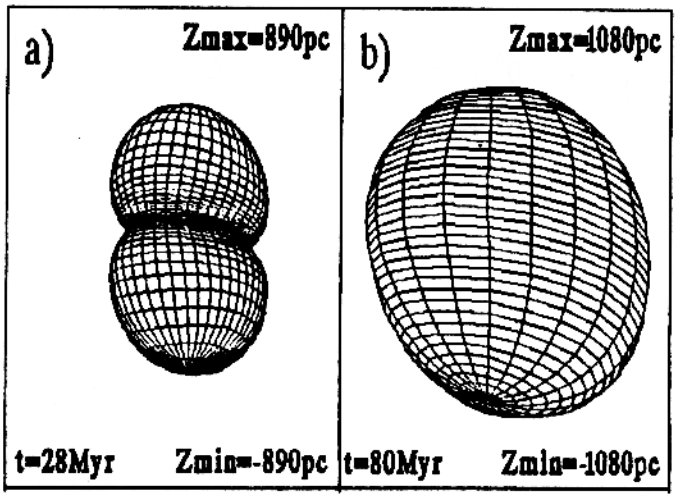

Figure 1 Superbubble morphology in different galaxies. Left: Galactic superbubble at R = 8.5 kpc with the energy supply rate L_{38} = 1.05 after 28 Myrs of expansion. Right: Superbubble in the HoII galaxy at R = 4.17 kpc with L_{38} = 0.34 after 80 Myrs of expansion.

2 GALACTIC SUPERSHELLS

Our numerical model is based on the 2.5-dimensional hydrodynamic code and includes effects of the gas density distribution, galactic rotation, gravity, and continuous energy input rate due to repeated supernova explosions inside the cavity. We also take into account the radiative losses of energy from the hot bubble interior and from the front of the radiative blast wave. Thermal evaporation of the cold dense shell is also allowed. The typical shape of the 3D expanding shell caused by the energy release in the midplane of the Galaxy is shown in Figure 1a. An hourglass remnant with a noticeable degree of deformation by the Galactic shear has appeared. After the bubble takes such a shape, both Z-component of gravity and pressure of the hot bubble interior couple their action to decelerate the lower parts of the shell. The Z-component of expansion velocity slows down and changes the direction near the midplane of the Galaxy. An expanding cusp, i.e. an expanding dense ring, is formed in the equatorial plane of the remnant. Mashchenko and Silich (1994) have shown that here the column number density may exceed the critical value N_c, that will prevent the internal shell layers from the penetration of the background UV radiation and allow the molecular gas formation. It was estimated that a molecular layer is likely to be developed within a very narrow (in Z-direction) part of the shell, only in the inner ($R < 15$ kpc) part of the Galaxy and if the OB-association is located below 100 pc from the Galactic plane. Nevertheless the mass of the interstellar gas compressed by a shock wave that can be transformed into molecular form may reach some $10^6 M_\odot$ (see Figure 2). The beginning of the gas infall into Galactic plane and cusp formation is, as we expect, the onset of the destruction of the shell as a coherent structure. The typical evolutionary time for

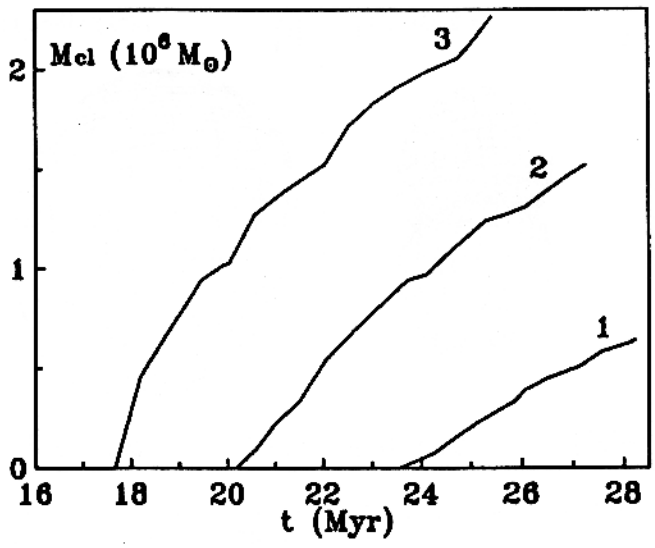

Figure 2 The mass of the shell material that can be transformed into molecular form. Curves 1, 2, 3 correspond to the energy release rate $L_{38} = 0.315$, 1.05 and 3.15. The bubble center is at 5 kpc from the Galactic center.

the onset of this process in the Galaxy is about 30 Myrs which restricts the development of structures highly elongated by the galactic shear. The ratio of the major supershell axis to the minor one does not exceed 2–3 at that time. Summary properties of the Galactic superbubbles with the energy input rate $L \approx 10^{38}$ ergs s^{-1}, that is from an OB-association with approximately 100 SNe explosions, are summarized in Table 2 (Silich *et al.* 1995). Here z_0 is the location of the OB-association above the Galactic plane, t_{max} is the time the calculations were ended at, z_{max} and z_{min} are the coordinates of the bubble top and bottom, L^x_{36} is the maximum X-ray luminosity in 10^{36} ergs s^{-1} units, T_{min} is the minimum temperature near the bubble center, M_{sh} is the mass of the shell, E^{OB}_{51} and E^k_{51} are the total energy released by the SN explosions and kinetic energy of the shell in 10^{51} ergs units.

3 SUPERSHELLS IN THE HoII GALAXY

A program to study ISM in dwarf galaxies was recently undertaken by Puche *et al.* (1992), Puche and Westpfahl (1994). The goal of the program is to determine the difference in the distribution of the components of the ISM in low mass systems and in grand design spirals. The Holmberg II galaxy is one from the sample for this study. It is a dwarf irregular companion of the M81 group which lies at a mean distance of 3.2 Mpc from us. A total kinematic mass of the galaxy was estimated as $M_{tot} \approx 2 \times 10^9 M_\odot$, with approximately 30% mass in the form of neutral hydrogen. The scale height of the HI layer derived from the measurements of the velocity

Table 2. Galactic superbubble parameters for energy input rate $L_{38} = 1.05$

z_0 pc	t_{max} Myr	z_{max} pc	z_{min} pc	L_{36}^x	T_{min} $10^6 K$	M_{sh} $10^6 M_\odot$	E_{51}^{OB}	E_{51}^k
				$R = 5$ kpc				
0	27.1	717	−717	1.1	2.2	2.75	90.	7.4
50	27.1	957	−376	1.2	2.3	2.59	90.	7.7
				$R = 8.5$ kpc				
0	30.3	916	−916	0.8	2.4	2.91	100.	5.4
50	30.0	1175	−499	0.8	2.5	2.60	100.	5.0
				$R = 15$ kpc				
0	30.1	1116	−1116	0.4	2.3	2.22	100.	7.8
50	30.1	1324	−884	0.4	2.3	2.14	100.	7.6

dispersion is $H = 625$ pc, that is much greater than the thickness of the gaseous disk in normal spirals. The orientation parameters, inclination i and position angle $P.A.$, were estimated to be $i \approx 40°$ and $P.A. \approx 177°$. The rotation curve displays a fast almost linear growth in the inner part of the galaxy and then becomes almost flat up to 7.5 kpc radius with the maximum value about 40 km s^{-1}.

The VLA observations have revealed 51 objects with characteristic sizes from 100 pc to 1700 pc which may be considered as expanding shells or holes in the HI column density distribution. Massive stars in the centers of large holes, H_α emission from the interior of the small holes and boundaries of the larger ones provide observational evidence for the mechanism of the correlated supernova explosions which is discussed here.

We tentatively assume that density of the stellar component of the HoII galaxy obeys King's distribution and is the dominant agent in the gravity field. Then Z-component of the gravitational field g_z and rotation velocity $V_{\rm rot}(r)$ may be expressed as follows:

$$g_z = -GM_c \frac{z}{\omega^3}\left[\ln\left(\frac{\omega}{r_c} + \sqrt{1+\left(\frac{\omega}{r_c}\right)^2}\right) - \frac{\omega}{r_c\sqrt{1+\left(\frac{\omega}{r_c}\right)^2}}\right], \qquad (1)$$

$$V_{\rm rot} = \left(\frac{GM_c}{r}\right)^{1/2}\left[\ln\left(\frac{r}{r_c} + \sqrt{1+\left(\frac{r}{r_c}\right)^2}\right) - \frac{r}{r_c\sqrt{1+\left(\frac{r}{r_c}\right)^2}}\right], \qquad (2)$$

where G is the gravity constant, $r = \sqrt{x^2+y^2}$ is the cylindrical and $\omega = \sqrt{x^2+y^2+z^2}$ is the spherical radii. The parameters M_c and r_c are defined from the rotation curve as follows: $M_c = 1.179 \times 10^9 M_\odot$ and $r_c = 929$ pc.

We have provided (Mashchenko and Silich, 1995) a set of numerical calculations to compare the theoretical model with the statistics of the HI holes distribution.

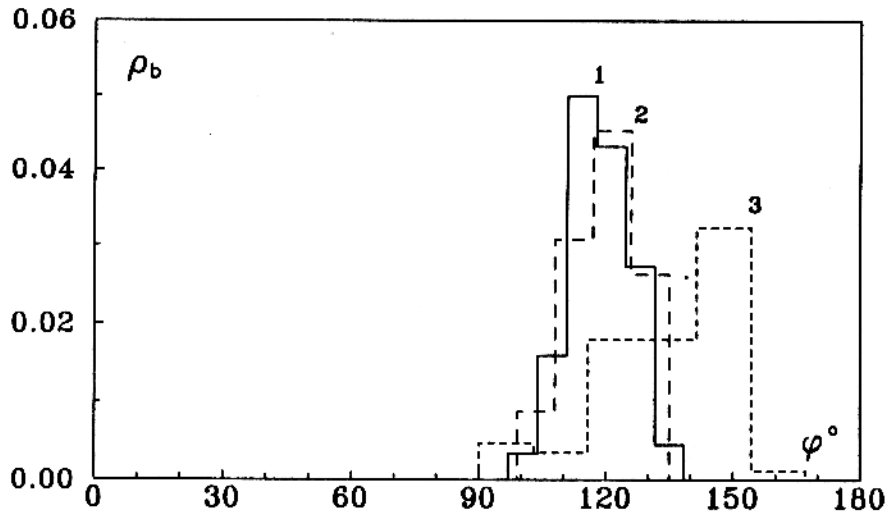

Figure 3 The calculated orientations of the HI holes in the HoII galaxy.

Our main goal was to compare the orientation of the main axes of the HI holes which follows from the numerical calculations with the observed one. To make it possible we have introduced the procedure of shell projection onto the plane of view. If x', y', z' is the frame of reference connected with the plane of view (center of galaxy is the point of reference), z' axis is directed to the observer, and z' axis is directed along the galaxy's line of nodes, then the HI column density N along the line of sight can be expressed as follows:

$$N(x', y') = \sum_j \frac{N_j}{|\cos \xi_j|} + \int n(x', y', z')\, dz'. \tag{3}$$

Here index j denotes intersection with different Lagrangian elements of the shell, ξ_j is the angle between the line of sight and the unit vector normal to the shell surface. The last term in the equation (3) gives the column density which is integrated in the galactic body outside the remnant.

The bubble evolution has been simulated for three galactocentric radii: R = 1.5 kpc, 4.17 kpc, and 6 kpc. The energy source was assumed to be located in the midplane of the galaxy and to provide energy input rate $L = 3.4 \times 10^{37}$ ergs s^{-1} that is due to approximately 30 supernova explosions during 30 Myrs. For every galactocentric radius nineteen polar angles, $\theta_i, \theta_{i+1} = \theta_i + 10°$ were considered, where θ is the angle between the X-axis and the radius-vector of the shell center. The theoretical maps of the column density distribution and parameters of the holes were calculated for every value of the polar angle θ with the time interval Δt = 10 Myrs for the inner part of the galaxy, R = 1.5 kpc, and Δt = 20 Myrs for R = 4.17 kpc and 6 kpc. Thus the HI maps and main observational parameters were generated for 285 shells with different ages and different location in the galaxy.

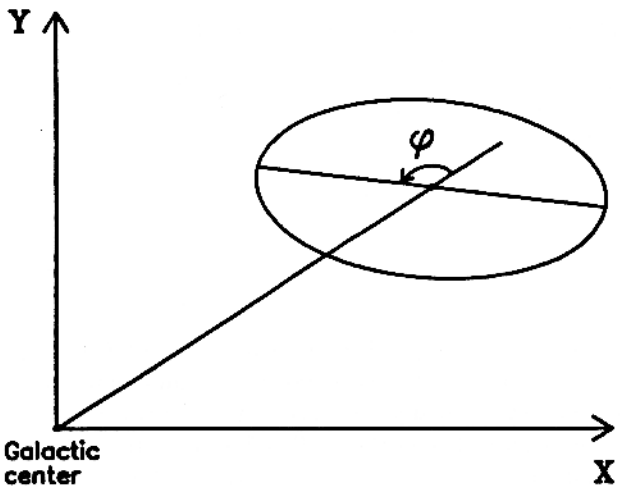

Figure 4 Scheme of the HoII orientation in the plane of view.

The typical shape of a neutral hydrogen shell in the HoII galaxy is shown in the Figure 1b. A larger thickness of the galactic gaseous disk and greater gradients in the radial gas distribution determine quite different morphology of the bubbles in the Holl galaxy in comparison with our own Galaxy. The distribution of the main axes of the HI holes that follows from the numerical simulations is presented in Figure 3 in the form of histograms for the density

$$\rho_b = \frac{1}{n}\frac{\Delta n_\varphi}{\Delta \varphi}. \tag{4}$$

Here n is the total number of holes the calculations have been done for at a particular galactocentric radius $R, \Delta n_\varphi$ is the number of holes with the main axes in the interval $\Delta\varphi$, where angle φ is defined in the scheme of Figure 4. The tangential orientation of the main axis corresponds to $\varphi = 90°$. The histograms 1, 2 and 3 are for the different positions of the hole center $R = 1.5$ kpc, 4.17 kpc, and 6 kpc. Note that the angle between the vector of the galactic angular momentum and the direction towards the observer i' was assumed to be equal to the inclination of the galaxy i: $i' = i = 40°$. Would spin of the galaxy be directed from the observer (angle $i' = 180° - i = 140°$), the angle φ should fall in the interval $0° \leq \varphi \leq 90°$. Thus we get a simple method allowing to distinguish between two possible directions of the galactic spin from the analysis of the HI holes' major axes distribution.

An observed value for the angle φ can be obtained from observations by Puche *et al.* (1992) as follows:

$$\varphi = P.A._h - \beta + 90°, \tag{5}$$

Table 3. The HI holes orientation in the HoII galaxy

Galactocentric distance (kpc)	Number of holes with $0° \leq \varphi \leq 90°$	Number of holes with $0° \leq \varphi \leq 180°$	α
0–7.5	24	20	45%
0–3.4	9	14	70%
3.4–7.5	15	6	95%

where $P.A._h$ is the position angle of the hole major axis, β is the polar angle of the hole center. Analysis of the observational data shows that major axes of the HI holes in the HoII galaxy are really concentrated in the third quadrant (see Table 3), but only in the outer part of the galaxy ($R > 3.4$ kpc). Here the χ^2 criterion rejects the main axes equipartition between the second and the third quadrants with the probability $\alpha = 95\%$. In the inner part of the galaxy, the distribution of the main axes of the holes is more homogeneous. We assume that different orientation of the HI holes comes from the interaction of shells with large-scale interstellar clouds or from the more frequent impacts between the shells in the inner part of the galaxy. Our calculations give evidence in favour of the Holl spin to be directed from the observer ($i' = 140°$). This conclusion is in contradiction with the results of Karachentsev (1989) who predicts from the analysis of the dust clouds distribution that the angle between the spin of the galaxy and direction towards the observer is $i' = 43° \pm 8°$. We are uncertain about the reasons for this discrepancy. Either Karachentsev's method does not operate well for the almost face-on galaxies, or some physical reasons restricts action of the galactic shear on the shell evolution.

4 SUMMARY

1. Shells, supershells and expanding bubbles among dominant features of the ISM in the normal spirals and dwarf irregular galaxies. It is likely that most of them can be explained by the correlated effects of interaction of OB stars and supernovae with the ambient medium. The morphology of the expanding superbubbles differs strongly in the massive spiral systems and dwarf irregular galaxies. This should lead to a different action of the bubble expansion on the transition between different phases of the ISM and on the process of the star formation.

2. Numerical simulations of the superbubbles evolution in the differentially rotating galactic disk allow to propose a simple method to determine the real (from two possible) direction of the galactic spin based on the analysis of the observed orientation of the HI holes' major axes in the plane of view.

3. Analysis of the neutral hydrogen column density distribution in the HoII galaxy displays a great variety in the HI holes orientation. We assume that

the difference between the observed and calculated orientations of the HI holes comes from the action of large-scale interstellar clouds or from impacts between the shells in the inner part of the galaxy.

4. Further development of the numerical models is necessary to take into account the action of the local inhomogeneities of the ISM, like interstellar clouds, and impacts between the neighbour shells on the evolution of the shell-like structure of the ISM in galaxies.

References

Bisnovatyi–Kogan, G. S. and Silich, S. A (1991) *Astron. Zh.* **68**, 749.
Brinks, E. (1990) In *The Interstellar Medium in Galaxies*, H. A. Thronson and J. M. Shull (eds.) (Netherlands: Kluwer Academic Publishers).
Cox, D. P. and Smith, B. W. (1974), *Ap. J.* **189**, L105.
Efremov,Yu.N. 1978, Pis'ma Astron. Zh., 4, 125.
Elmegreen, B. G. (1985) *Protostars & Planets II.*
Heiles, C. (1979) *Ap. J.* **229**, 533.
Hindman, J. V. (1967) *Aust. J. Phys.* **20**, 147.
Karachentsev, I. D. (1989) *Astron. Zh.* **66**, 907.
Mashchenko, S. Ya. and Silich, S. A. (1994) *Astron. Zh.* **71**, 237.
Mashchenko, S. Ya. and Silich, S. A. (1995) *Astron. Zh.* (in press).
McCray, R. and Kafatos, M. (1987) *Ap. J.* **317**, 190.
Palous, J. (1990) *IAU Symp. No. 144, Poster proceeding* 101.
Puche, D., Westpfahl, D., Brinks, E., and Roy, J.-R. (1992), *A. J.* **103**, 1841.
Puche, D. and Westpfahl, D. (1994), *A. J.* (in press).
Silich, S. A. (1992) *Astrophys. Spase Sci.* **195**, 317.
Silich, S. A., Franko, J., Palous, J., and Tenorio–Tagle, G. (1995) (in preparation).
Tenorio–Tagle, G. (1980) *A&A* **8**, 61.
Tenorio–Tagle, G., Bodenheimer, P., Rozyczka, M., and Franco, J. (1986) *A&A* **170**, 107.
Tenorio–Tagle, G. and Bodenheimer, P. (1988) *ARA&A* **26**, 145.
Tomisaka, K., Habe, A., and Ikeuchi, S. (1981) *Astrophys. Space Sci.* **78**, 273.